Neural Network Model for Breast Tissue Thickness Estimation

Henna Jethani[#1], Milica Popović[*2], Zoya Popović[#3]
[#]University of Colorado at Boulder, USA
[*]McGill University, Canada
[1]henna.jethani@colorado.edu, [2]milica.popovich@mcgill.ca,[3]zoya@colorado.edu

***Abstract*— This paper explores the use of optimization methods to estimate thicknesses of subcutaneous tissues using a non-invasive near-field antenna with microwave low-power reflectometry from 2–13.5 GHz. An application is in breast cancer detection at microwave frequencies. The initial model assumes a planar tissue stack and is implemented with a Long Short-Term Memory (LSTM) neural network trained on full-wave electromagnetic simulation data. Tissue phantoms for skin, fat and muscle with 2 and 3 layers are used for experimental validation. The model developed for this paper predicts thicknesses of a stackup of Playdough, Rogers Duroid 6010 and a commercial skin phantom within 7%, 41%, and 24% respectively, with a neural network loss value of 0.29. This preliminary model is a proof of concept for a higher fidelity model that can additionally predict dispersive permittivities and conductivities of layered tissues.**

***Keywords*— Neural networks, RNN, LSTM, custom loss function, electromagnetics, tissue properties.**

I. Introduction

In this paper we address the problem of *in-situ* measurement and estimation of sub-cutaneous tissue layer electrical properties at microwave frequencies. The knowledge of thicknesses, permittivities and conductivities of tissue layers is needed for design of e.g. antennas for body-area communication networks, wireless powering of implants and wearable textile antennas, e.g. [1], [2]. The motivation for the work in this paper is breast cancer detection using microwaves, illustrated in Fig. 1, researched worldwide in the past few decades [3]. All the methods addressing this application use the same underlying hypothesis: due to the different water content, there is an inherent dielectric contrast between healthy and cancerous breast tissues at microwave frequencies [4]. Hence, when a low-power microwave signal is launched at the skin surface, the backscattered signal collected on the skin surface contains information on the subcutaneous dielectric structure, including any tumorous anomalies.

This promising approach encounters a number of well-documented challenges. First, the variation in the dielectric properties directly implies the variation in the detectability levels, as the signal must be low-power for safety considerations. Second, women's tissue densities vary, and this medically-categorized variation implies a subtle change of dielectric properties from one individual to another. Finally, the lossy and high-permittivity skin, the first layer through which the wave propagates, must be properly accounted for, both at the level of hardware design and at the signal-processing stage [6]. Having an accurate estimate of near-surface tissue

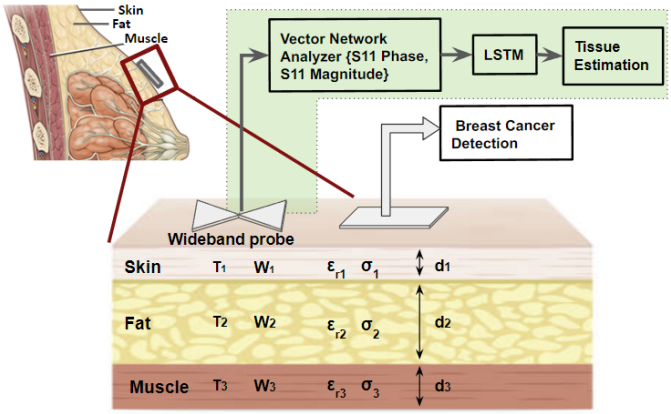

Fig. 1. Illustration of breast tissue estimation that can assist breast cancer detection. By nature of low-power, safe detection of breast cancer, microwaves do not reach the muscle of the chest wall. To determine the layer properties $(d_i, \epsilon_{ri}, \sigma_i)$ a wideband antenna collects reflectometry data from a vector network analyzer (VNA) from 2 to 13.5 GHz, fed into a LSTM algorithm. The focus of this paper (indicated in green) is to determine the tissue layer thicknesses d_i, and muscle is included for general tissue estimation proof-of-concept [5].

layers will help in calibrating the microwave imaging process to each particular patient. Factors including age, race, gender, and genetic history affect the composition of tissues in the human body and limited data exists in the literature on body composition across a diverse population. For example, [7] reports that although research groups have attempted to cover the variation in skin structure and function across diverse groups, these studies remain limited in their sample size or they focus on interindividual variations in skin quality and overlook racial differences.

In [8], broadband 0.5–20 GHz characterization of breast tissue is performed using a coaxial probe. Although this data can be helpful, a practical application requires a fast measurement of tissue properties at a specific place where breast-cancer imaging data is acquired for a one-time calibration. To determine the layer properties (thickness d_i, relative permittivity ϵ_{ri} and conductivity σ_i) a wideband near-field antenna collects 2–13.5 GHz reflectometry data with a vector network analyzer (VNA), which is then fed into a Long Short-Term Memory (LSTM) model. Layer properties are different across body types, requiring "model calibration". Permittivity and conductivity are frequency-dependent while thickness is frequency-independent, and therefore we start the calibration using a neural network model to solve for tissue

thickness of each layer in a 2-layer and 3-layer stackup. The training data from HFSS are first collected using a simulation of the complex reflection coefficient (S_{11}) at the port of a broadband (2–13.5 GHz) near-field bow-tie antenna [9] against a stackup that is parameterized for varying layer thicknesses. The LSTM model is composed in Python using the Keras library. The validation step occurs when the model is used to make a prediction on the VNA reflection coefficient data collected from the antenna placed on a comparable tissue phantom stackup. An example electric field vector magnitude distribution of the near-field antenna at 2.45 GHz is presented in Fig. 2, for 1 W of incident power. An image of the antenna numerical model is shown in the same figure. The near-field distribution does not change significantly across frequencies where the antenna is well matched.

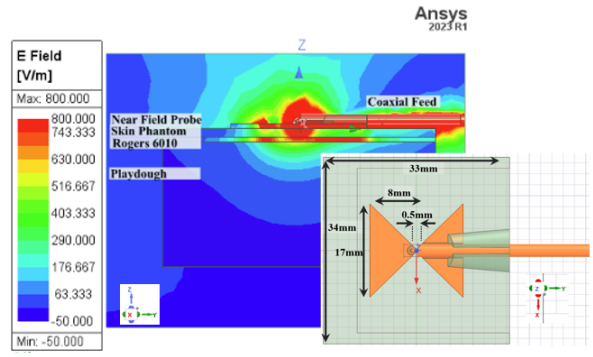

Tissue	ϵ	$\sigma(S/m)$	Thickness Range (mm)
Skin Phantom (Speag)	24.3	1.98	1 to 3
Duroid (Rogers 6010)	10.2	-	1 to 3
Playdough	27	7	25 to 35

Fig. 2. Top is a plot of electric field magnitude at 2.45 GHz for the broadband probe against a three layer stackup of 2.25 mm thick skin phantom, 1.91 mm thick Rogers 6010, and 30 mm thick Playdough. Numerical model of the probe is shown in the bottom right corner. Bottom is a table of the electromagnetic properties and thickness ranges used in simulation.

For the phantoms, we used materials whose electromagnetic properties have been characterized in a lab environment and that are readily available to ensure reproducibility of results. The near-field antenna is simulated with two phantom tissue stackups: (1) a commercial skin phantom manufactured by Speag [10], a low-loss microwave substrate (Rogers Duroid 6010) simulating fat, and Playdough; and (2) the skin phantom and Playdough, known in the bio-electromagnetic community to be a reasonable muscle phantom. Frequency-dependent permitivity and conductivity are defined in the model for skin phantom and Playdough. The dispersive permittivity and conductivity values are used from [9]. Simulations are executed for the two-layer and three-layer stackups over a range of thicknesses. The results include $|S_{11}|$ and $\angle S_{11}$ per iteration of thickness, per layer over the frequency range of 2–13.5 GHz. The training data set is composed of 447 permutations of layer thicknesses. The data is exported from HFSS to CSV files to be used as training data for the LSTM code. Fig. 3 exhibits a comparison between an iteration of simulation data with the corresponding

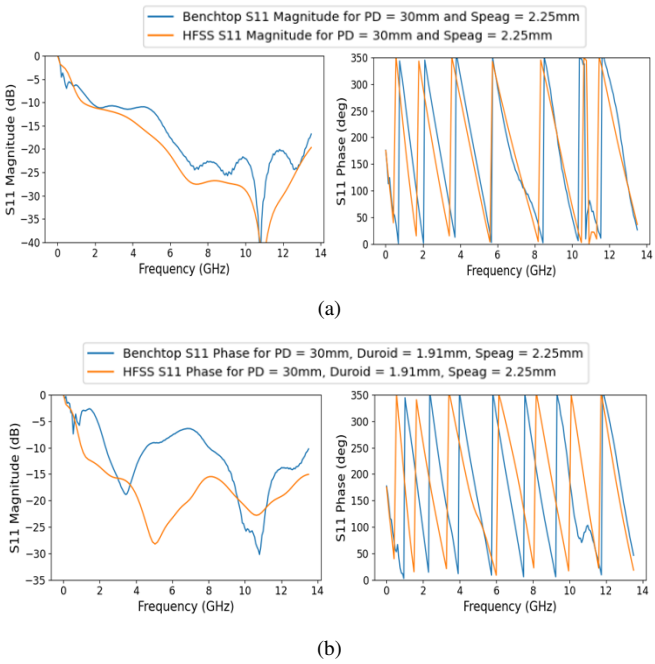

Fig. 3. (a) Experimental and simulated $|S_{11}|$ and $\angle S_{11}$ for a two-layer stackup of Playdough and commercial tissue phantom, Speag. (b) Experimental and simulated $|S_{11}|$ and $\angle S_{11}$ for a three-layer stackup of Playdough, Rogers Duroid 6010, and commercial skin phantom from Speag. Orange lines represent HFSS data and blue lines represent experimental data.

experimental data, demonstrating that simulation data is a valid method for training the LSTM model.

II. Neural Network Architecture

Prior to selecting LSTM, both Multi Level Perceptron (MLP) and Recurrent Neural Networks (RNN) were considered when determining the architecture to apply to the internal thermometry calibration problem. Commonly, MLPs are applied to biomedical problems, however they are used when the predictions are based off static data. Since the goal is to predict frequency-dependent data and the training data is over frequency, the neural network must capture sequential patterns to make predictions [11]. LSTMs are a specific type of RNN that are used to recognize long-term dependencies in temporal data [12]. The X training data set is composed of frequency, $|S_{11}|$, and $\angle S_{11}$. The Y data is composed of the number of layers and their thicknesses. Each feature is scaled by the minimum and maximum values of that feature. In the model, 70 % of the data is used for training and 30 % is used for test. The sequences of data are randomly shuffled when training and testing datasets were configured.

The initial layer of the LSTM model consists of 50 units accompanied with the 'Tanh' activitation function, which offers larger gradients around its zero center, which can capture minor changes in the sequential data. Tanh is chosen over Rectified Linear Unit (ReLU) to avoid the "dying ReLU" problem, during which negative inputs can lead to zero gradients resulting in inactive neurons [13]. This must be

avoided in order for intricacies of the temporal data to be detected by the LSTM.

Three dense layers follow the initial layer, concluding with the final layer consisting of four units, addressing the four output parameters: number of layers; Playdough thickness; Rogers 6010 thickness; and Speag skin phantom thickness. Dropout layers are additionally incorporated for regularization and to prevent overfitting [14].

A custom loss function addresses the physical constraints of the problem as well as minimizes prediction errors. The loss function incorporates the requirements that the number of layers prediction must be an integer and that thickness values are non-negative and within a reasonable band corresponding to the material nature of that layer. The loss function is composed of a mean squared error (MSE) term with penalty terms for conditions including non-integer values for number of layers and negative values for layer thicknesses [15]. The penalty for non-integer values is determined by calculating the absolute difference between the number of predicted layers and the closest integer value. Then penalties are calculated for negative thicknesses, which cannot physically exist. Multiplying the penalty values with coefficients allows the model to prioritize penalties between the layer predictions. Coefficients were determined by trial and error. Combining the coefficients with the penalties provides a total loss function that is used by the model to modify weights during training. In cases when the experimental data does not cover the complete frequency range of the training data, a linear interpolation with extrapolation for data outside the given frequency range is incorporated in the model.

III. Results and Experimental Validation

When evaluating the performance of the model, a few metrics are observed including the loss obtained as well as the predictions that the model makes for benchtop measurements. A model loss of 0.29 is obtained over the training process of 200 epochs, indicating that the model is performing at an adequate standard.

In addition to evaluating the performance of the model from simulation data, we used the model to make predictions on physical data obtained from a benchtop setup. A 10 MHz–13.5 GHz VNA is used with the near-field bow-tie antenna modeled in HFSS against a stackup of Playdough, Rogers 6010 and Speag skin phantom. Two physical stackup setups are used for this preliminary verification phase. The first is a two-layer model composed of the skin phantom and Playdough and the second uses all three materials. The resulting $|S_{11}|$ and $\angle S_{11}$ values from the VNA are used to make predictions on the thickness of each layer as well as the number of layers. The comparison between the benchtop values and the values predicted by the neural network model are shown in Table III. Here rounding to an integer is used for the number of layer prediction.

Variation between the true values and predicted values are likely a result from the deviation between the benchtop S_{11} data compared to that obtained from HFSS as shown in Fig. 3. This could be due to a number of factors, e.g., the materials are not exact to their datasheets, or the Playdough experienced some drying from the time when it was fitted.

Table 1. Actual parameters of the experimental setup compared to the LSTM predictions of the experimental setup.

Test Type	Predicted No. of Layers	Layer Type	True Thickness [mm]	Predicted Thickness [mm]
2 Layer	2.32 → **2**	Playdough	30	28.10
		Rogers 6010	0	0.56
		Speag	2.25	1.71
3 Layer	2.75 → **3**	Playdough	30	29.783
		Rogers 6010	1.91	1.109
		Speag	2.25	1.86

In summary, this research shows that thickness for 2 and 3-layer experimental stackups of Playdough, Rogers Duroid 6010, and commercial skin tissue phantoms can be predicted within 7%, 41%, and 24% respectively, using the LSTM model described in this paper. Future work will extend the model to predict dispersive permittivity and conductivity.

References

[1] S. Movassaghi, M. Abolhasan, J. Lipman, D. Smith, and A. Jamalipour, "Wireless body area networks: A survey," *IEEE Communications surveys & tutorials*, vol. 16, no. 3, pp. 1658–1686, 2014.

[2] P. Salonen, Y. Rahmat-Samii, and M. Kivikoski, "Wearable antennas in the vicinity of human body," in *IEEE Antennas and Propagation Society Symposium, 2004.*, vol. 1, 2004, pp. 467–470 Vol.1.

[3] A. Modiri, S. Goudreau, A. Rahimi, and K. Kiasaleh, "Review of breast screening: Toward clinical realization of microwave imaging," *Medical physics*, vol. 44, no. 12, pp. e446–e458, 2017.

[4] A. Martellosio and et al., "Dielectric properties characterization from 0.5 to 50 ghz of breast cancer tissues," *IEEE Transactions on Microwave Theory and Techniques*, vol. 65, no. 3, pp. 998–1011, 2016.

[5] Breast ultrasound. https://www.hopkinsmedicine.org/health/treatment-tests-and-therapies/breast-ultrasound.

[6] P. Meaney, S. Geimer, A. Golnabi, and K. Paulsen, "Impact of skin on microwave tomography in the lossy coupling medium," *Sensors*, vol. 22, no. 19, p. 7353, 2022.

[7] A. V. Rawlings, "Ethnic skin types: are there differences in skin structure and function?" *International Journal of Cosmetic Science*, vol. 28, no. 2, pp. 79–93, 2006.

[8] M. Lazebnik and et al., "A large-scale study of the ultrawideband microwave dielectric properties of normal breast tissue obtained from reduction surgeries," *Physics in Medicine Biology*, vol. 52, p. 2637, apr 2007.

[9] R. Streeter, "High-resolution deep-tissue microwave thermometry," Ph.D. dissertation, University of Colorado at Boulder, 2023.

[10] SPEAG. Swiss speag. https://speag.swiss/. Accessed on October 7, 2023.

[11] S. Hochreiter and J. Schmidhuber, "Long short-term memory," *Neural computation*, vol. 9, pp. 1735–80, 12 1997.

[12] B. Lindemann, T. Müller, H. Vietz, N. Jazdi, and M. Weyrich, "A survey on long short-term memory networks for time series prediction," *Procedia CIRP*, vol. 99, pp. 650–655, 2021. [Online]. Available: https://www.sciencedirect.com/science/article/pii/S2212827121003796

[13] L. Lu, Y. Shin, Y. Su, and G. Karniadakis, "Dying relu and initialization: Theory and numerical examples," 03 2019.

[14] SaturnCloud, "How to implement dropout in lstm neural networks with tensorflow," https://saturncloud.io/blog/how-to-implement-dropout-in-lstm-neural-networks-with-tensorflow/, 2023.

[15] E.-J. Skinner. (2023) Custom loss. https://towardsdatascience.com/creating-a-innovative-custom-loss-function-in-python-using-tensorflow-and-fitting-a-lstm-model-ded222efbc89.